Refinements of On-The-Fly Doppler Broadening via Gauss-Hermite Quadrature in Monte Carlo Reactor Analysis

YuGwon Jo and Nam Zin Cho*
Korea Advanced Institute of Science and Technology (KAIST)
291 Daehak-ro, Yuseong-gu, Daejeon, Korea 34141
**nzcho@kaist.ac.kr*

1. Introduction

For the high-fidelity reactor analysis, a continuous-energy Monte Carlo (MC) neutron transport code requires temperature dependent cross sections. Usually, the cross sections are pre-generated as piecewise linear functions in energy at fixed temperatures, where the temperature dependence of a cross section is treated by the SIGMA1 algorithm [1] in the BROADR module of NJOY [2].

The simplest approach to the treatment of temperature dependence of cross sections is interpolation of the pre-generated cross sections [3]. However, this approach requires excessive memory (around 130 GB) to cover temperatures from 0K to 3000K. The other approach is on-the-fly (OTF) Doppler broadening, which provides temperature-effective cross sections during simulation of neutron transport. Recently, several OTF methods have been proposed [4-7].

One of the OTF methods, the windowed multipole method [7] shows remarkable performance in terms of both memory and computing time. However, for some nuclides, resonance parameters are not provided in the ENDF database, which makes it impossible to apply the windowed multipole method.

On the other hand, Dean, et al. [4] proposed to apply the Gauss-Hermite quadrature (GHQ) to evaluate the Doppler broadened cross sections. Compared to the two-point Gauss-Legendre quadrature (GLQ) algorithm [8] and the SIGMA1 algorithm, the GHQ algorithm significantly reduces the computing times, while it shows oscillatory error (with maximum relative error of 2%) in the low energy range ($E < 16kT/A$) [4,9]. To avoid such accuracy degradation, Ref. 9 also applied the SIGMA1 algorithm to the low energy range, but at the expense of computing times.

In this paper, the GHQ algorithm is refined in two aspects. One is that the Doppler broadened cross section in the low energy range is estimated by the two variations of GHQ (GHQ1 and GHQ2) and the two-point GLQ for both accuracy and computational efficiency. The other is a refined cross-section table lookup procedure for GHQ to reduce computing times. The numerical results show that these refinements lead to significantly improved performance.

2. Gauss-Hermite Quadrature (GHQ) Algorithm for Doppler Broadening

The effective cross section at temperature T can be written as [1] :

$$\sigma(y,T) = \frac{1}{y^2\sqrt{\pi}} \int_0^\infty dx\, x^2 \sigma\left(x,T_0\right)\left[e^{-(x-y)^2} - e^{-(x+y)^2} \right], \quad (1)$$

where $x^2 = \alpha E_r$, $y^2 = \alpha E$, $\alpha = \dfrac{A}{k\left(T-T_0\right)}$,

E_r is relative incident neutron energy with respect to target, E is incident neutron energy, A is the ratio of the target mass to the neutron mass, and T_0 is the base temperature at which the cross section is provided in piecewise-linear tabulation.

It is conventional to split Eq. (1) in two separate parts:

$$\sigma(y,T) = \sigma^*(y,T) - \sigma^*(-y,T) , \quad (2)$$

where $\sigma^*(y,T)$ and $\sigma^*(-y,T)$ are defined as:

$$\sigma^*(y,T) = \frac{1}{y^2\sqrt{\pi}} \int_0^\infty dx\, x^2 \sigma(x,T_0) e^{-(x-y)^2} , \quad (3a)$$

$$\sigma^*(-y,T) = \frac{1}{y^2\sqrt{\pi}} \int_0^\infty dx\, x^2 \sigma(x,T_0) e^{-(x+y)^2} . \quad (3b)$$

For $y \geq 4$, we only need to perform the integration for $\sigma^*(y,T)$ in Eq. (2), because $\sigma^*(-y,T)$ becomes negligible. Eq. (3a) is rewritten into a suitable form for the Gauss-Hermite quadrature (GHQ) [4,9] using a change of variable from x to $z = x - y$ as:

$$\sigma^*(y,T) = \frac{1}{y^2\sqrt{\pi}} \int_{-y}^\infty dz\, e^{-z^2} (z+y)^2 \sigma(z+y,T_0) \quad (4a)$$

$$\simeq \frac{1}{y^2\sqrt{\pi}} \int_{-\infty}^\infty dz\, e^{-z^2} (z+y)^2 \sigma(z+y,T_0) \quad (4b)$$

$$\simeq \frac{1}{y^2\sqrt{\pi}} \sum_{k=1}^{N} w_k (z_k+y)^2 \sigma(z_k+y,T_0) , \quad (4c)$$

where z_k and w_k are the nodes and weights of GHQ on an infinite interval, respectively, and N is the quadrature order, which is chosen as 16 in this study. Note that for $y \geq 4$, the lower limit of integration, $-y$ in Eq. (4a), can be approximated as $-\infty$ in Eq. (4b) without loss of significant accuracy, due to the e^{-z^2} function.

For $y < 4$, the mismatch of the lower limits of integration for $\sigma^*(y,T)$ causes significant errors. Furthermore, $\sigma^*(-y,T)$ in Eq. (2) is not negligible anymore, and thus, it should be also estimated. The estimation of $\sigma^*(-y,T)$ using GHQ based on a change of variable from x to $z = x + y$ could be more erroneous, due to the fact that the lower limit of integration y cannot be approximated as $-\infty$. Therefore, it requires a special treatment in the low energy range (i.e., $y < 4$) to retain accuracy. For this purpose, three algorithms are presented in Section 3.

3. Doppler Broadening Algorithms in Low Energy Range

In this section, three different Doppler broadening algorithms are presented for the low energy range ($y < 4$).

3.1 GHQ1 algorithm

Similarly to Section 2, GHQ based on a change of variable from x to $z = x - y$ is applied to Eq. (1) as:

$$\sigma(y,T) = \frac{1}{y^2\sqrt{\pi}} \int_{-y}^{\infty} dz\ (e^{-z^2} \times (z+y)^2 \sigma(z+y,T_0)(1-e^{-4y(z+y)})) \quad (5a)$$

$$\simeq \frac{1}{y^2\sqrt{\pi}} \sum_{k=1}^{N} (w_k (z_k+y)^2 \sigma(z_k+y,T_0) \times (1-e^{-4y(z_k+y)})) \ . \quad (5b)$$

In the GHQ1 algorithm, $\sigma^*(y,T)$ and $\sigma^*(-y,T)$ are not separately estimated, while the evaluation of the exponential function at each GHQ node z_k is required. It is noted that when $z_k + y < 0$ in Eq. (5b), the quadrature summations are skipped. It will be shown in Section 5.1 that the GHQ1 algorithm shows significant oscillatory errors in the low energy range, similarly to the previous study [4].

3.2 Two-point GLQ algorithm

For $y < 4$, the two-point GLQ algorithm [8] is applied to perform the integrations in Eqs. (3a,b) to retain accuracy. The GLQ algorithm requires evaluations of exponential functions for each piecewise linear energy grid interval, which take heavy computational burdens, compared to the GHQ algorithm. In this paper, we use two-point GLQ. One can think of a one-point GLQ algorithm with merging several piecewise linear energy grids to reduce the computational burdens.

3.3 GHQ2 algorithm

GHQ on a semi-infinite interval is applied to Eq. (1) as:

$$\sigma(y,T) = \frac{e^{-y^2}}{y^2\sqrt{\pi}} \int_0^{\infty} dx\ e^{-x^2} x^2 \sigma(x,T_0)(e^{2xy} - e^{-2xy}) \quad (6a)$$

$$\simeq \frac{e^{-y^2}}{y^2\sqrt{\pi}} \sum_{k=1}^{\tilde{N}} \tilde{w}_k x_k^2 \sigma(x_k,T_0)(e^{2x_k y} - e^{-2x_k y}) \ , \quad (6b)$$

where x_k and $\tilde{w}_k$ are the nodes and weights of GHQ on a semi-infinite interval, respectively. $\tilde{N}$ is chosen as 16 to avoid $x_k = 0$ and maintain accuracy of the effective cross section near $y = 4$. It is noted that, for each node x_k, one evaluation of the exponential function is required.

4. Refined Cross-Section Table Lookup for GHQ

When we calculate the effective cross section using GHQ, cross-section table lookups take significant computational burdens, because we need to look up cross sections for each GHQ node. For example, 16 times of cross section table lookups are required for GHQ of order 16.

To reduce the computing times for cross-section table lookups, we can use the logarithmic hash-table [10]. On top of this basic hash-table, we can narrow the energy range for cross section table lookups by updating the lower energy bound and the upper energy bound during the quadrature summation.

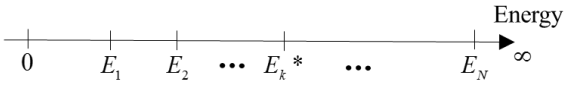

$*E_k = \frac{(z_k+y)^2}{\alpha}$ and z_k = the k-th GHQ node for $k = 1$, to N.

Fig. 1. Energies corresponding to GHQ nodes.

The following is the refined cross section table lookup procedure for GHQ using Fig. 1:

1) Search energy grid indices of E_1 and E_N using the logarithmic hash-table.
2) Set lower bound and upper bound of energies as E_1 and E_N, respectively, and search for the energy grid index of E_2.
3) Update the lower bound energy as E_2 and search for E_3.
4) Continue update of the lower bound energy to narrow the energy range for the next energy grid search.

5. Numerical Results

5.1 Doppler Broadening of Total Cross Section of U-238

The total cross section of U-238 at 600K, 900K, and 1200K is obtained at each energy grid point, where the cross section at 293K provided by NJOY is used for Doppler broadening. The reference total cross sections for these temperatures are obtained from the SIGMA1 algorithm. The GHQ algorithm is used for Doppler broadening for $y \geq 4$ while three different Doppler broadening algorithms (GHQ1, Two-point GLQ, and GHQ2) are used for $y < 4$. Note that, for energy above 1 MeV or above the resolved resonance energy range, Doppler broadening is turned off. In case of U-238, the lower bound of the unresolved resonance range is 20 keV.

Figures 2, 3, and 4 show relative errors in the effective total cross sections of U-238 at 600K, 900K, and 1200K, respectively. For $y < 4$, there are oscillatory errors in the GHQ1 algorithm, while the relative errors in both two-point GLQ algorithm and GHQ2 algorithm are almost zero. Figure 5 compares computing times for the Doppler broadening algorithms for $y < 4$. In terms of both accuracy and computing times, GHQ2 shows the best performance for the low energy range.

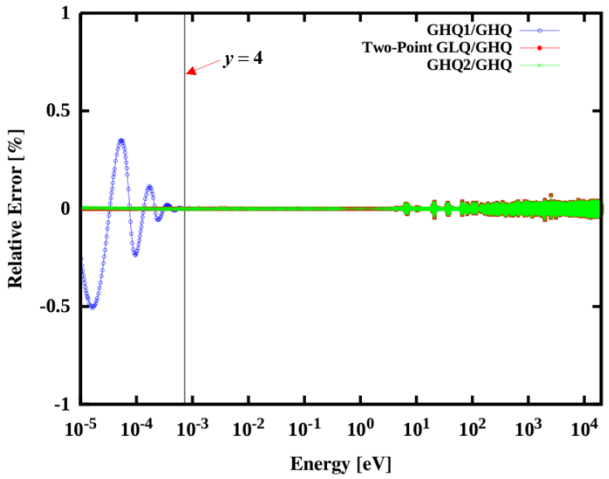

Fig. 2. Relative errors in total cross sections of U^{238} at 600K (relative to SIGMA1).

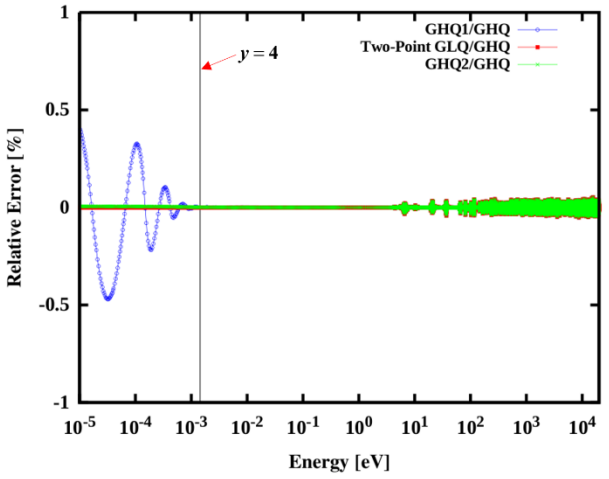

Fig. 3. Relative errors in total cross sections of U^{238} at 900K (relative to SIGMA1).

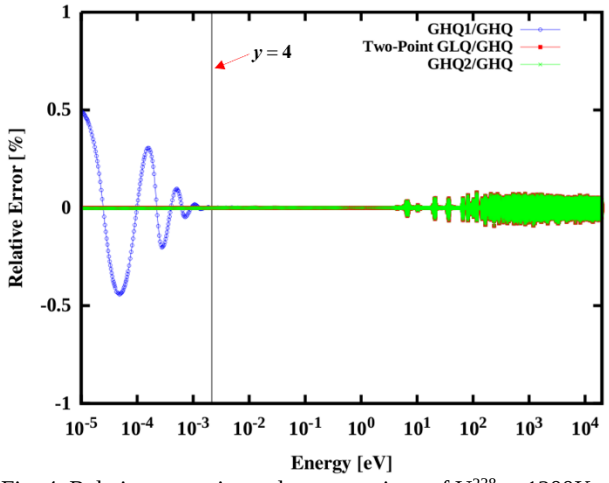

Fig. 4. Relative errors in total cross sections of U^{238} at 1200K (relative to SIGMA1).

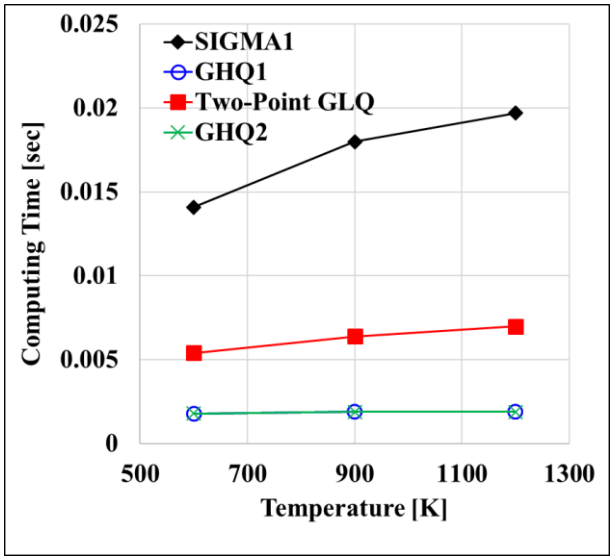

Fig. 5. Comparison of computing times for Doppler broadening algorithms for $y < 4$, where computing times are measured on Xeon® CPU X5670 @ 2.93 GHz.

5.2 OTF Doppler Broadening in UO_2 Pin-Cell Problem

The UO_2 pin-cell test problem is shown in Fig. 6. The temperatures of all the materials are set as 600K. We perform MC simulation with OTF Doppler broadening based on the continuous-energy nuclear data (ENDF/B-VII.0) at 293K. For Doppler broadening, the GHQ algorithm is used for $y \geq 4$, while the three different Doppler broadening algorithms; GHQ1, Two-point GLQ, and GHQ2 are used for $y < 4$. The continuous-energy MC simulations are performed by the in-house MC code, McBOX [11]. The calculational conditions are 200,000 histories/cycle, 10 inactive cycles, and 100 active cycles.

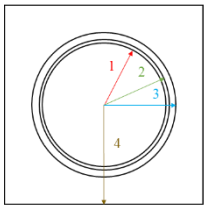

Arrow	Length[cm]	Material	Density [g/cc]
1	0.39218	UO_2	10.30166
2	0.40005	Helium	1.598E-3
3	0.45720	Zircaloy	6.55
4	0.63000	Water	0.740582

Fig. 6. UO_2 pin-cell test problem containing total 32 isotopes at 600K.

Table I compares the multiplication factors and computing times of MC simulations using different OTF Doppler broadening algorithms. All the multiplication factors shown in Table I agree well within 1σ. Both "GHQ1/GHQ" algorithm and "GHQ2/GHQ" algorithm are 4 times faster than "Two-point GLQ/GHQ" algorithm, while they are 6~7 times slower than the reference calculation, where the reference calculation means that MC simulation by the cross sections pre-generated by NJOY (SIGMA1 algorithm) at 600K.

Table I. Comparisons of k_{eff}'s and computing times

OTF Methods	k_{eff} (σ)	Computing Times [sec]	Ratio of Computing Times
GHQ1/GHQ	1.22383 (13.2 pcm)	234	6.87
Two-Point GLQ/GHQ	1.22384 (15.0 pcm)	875	25.75
GHQ2/GHQ	1.22374 (13.5 pcm)	221	6.50
Reference*	1.22372 (14.3 pcm)	34	1.00

*Reference is obtained from MC simulation by the cross sections pre-generated by NJOY (SIGMA1 algorithm) at 600K.

6. Summary and Conclusions

In this paper, the on-the-fly (OTF) Doppler broadening algorithm via Gauss-Hermite quadrature (GHQ) is refined. For the low energy range ($y < 4$), the effective cross section is estimated by the GHQ2 algorithm to improve both accuracy and computational efficiency. To further reduce the computing times for Doppler broadening, a procedure of cross-section table lookups for the GHQ algorithm is also refined. From the numerical results, we have shown that the GHQ2 algorithm removes oscillatory errors in the low energy range, which appear in the GHQ1 algorithm, while the computing time of the GHQ2 algorithm is much faster than that of the two-point GLQ algorithm.

In conclusion, the "GHQ2/GHQ" algorithm (GHQ2 for $y < 4$ and GHQ for $y \geq 4$) with the refined cross-section table lookup procedure can be an efficient and accurate OTF Doppler broadening algorithm for MC simulations, when the cross section data is piecewise linearly tabulated.

Acknowledgements

This work was supported in part by KUSTAR-KAIST Institute (KKI), Korea, under the R&D program (N1117dd0014) supervised by KAIST. This work was also supported in part by a National Research Foundation grant funded by the Korean government (Ministry of Science, ICT and Future Planning) (No. 2015M2B2A9029928).

References

[1] D.E. Cullen and C. R. Weisbin, "Exact Doppler broadening of tabulated cross sections," *Nucl. Sci. Eng.*, **60**, 199-229 (1976).
[2] R.E. MacFarlane, et al., "The NJOY nuclear data processing system, version 2012," Technical Report LA-UR-12-27079, Los Aalamos National Laboratory, 2012.
[3] T.H. Trumbull, "Treatment of nuclear data for transport problems containing detailed temperature distributions," *Nucl. Technol.*, **156**, 75-76 (2006).
[4] C. Dean, et al., "Validation of run-time Doppler broadening in MONK with JEFF3.1," *J. Kor. Phys. Soc.*, **59**, 1162-1165 (2011).
[5] G. Yesilyurt, et al., "On-the-fly Doppler broadening for Monte Carlo codes," *Nucl. Sci. Eng.*, **171**, 239-257 (2012).
[6] T. Viitanen and J. Leppanen, "Explicit treatment of thermal motion in continuous-energy Monte Carlo tracking routines," *Nucl. Sci. Eng.*, **171**, 165-173 (2012).
[7] B. Forget, et al., "Direct Doppler broadening in Monte Carlo simulations using the multipole representation," *Ann. Nucl. Energy*, **64**, 78-85 (2014).
[8] S. Li, et al., "Research on fast-Doppler-broadening of neutron cross sections," *PHYSOR 2012*, Knosville, TN, USA, April 15-20, 2012.
[9] P.K. Romano and T.H. Trumbull, "Comparison of algorithms for Doppler broadening pointwise tabulated cross section," *Ann. Nucl. Energy*, **75**, 358-364 (2015).
[10] F. B. Brown, "New hash-based energy lookup algorithm for Monte Carlo codes," *Trans. Am. Nucl. Soc.*, **111**, 659-662 (2014).
[11] Y.G. Jo and N.Z. Cho, "Users' Manual for McBOX–A Monte Carlo Code Version 1," Korea Advanced Institute of Science and Technology, NURAPT-2016-03 (April 2016).